*Computers and Concrete, Vol. 10, No. 6 (2012) 631-647*
DOI: http://dx.doi.org/10.12989/cac.2012.10.6.631 

# Application of Fuller's ideal curve and error function to making high performance concrete using rice husk ash

Chao-Lung Hwang*, Le Anh-Tuan Bui and Chun-Tsun Chen

*Department of Construction Engineering, National Taiwan University of Science and Technology 43, Keelung Rd., Sec. 4, Taipei 106, Taiwan, R.O.C*

*(Received December 15, 2011, Revised April 27, 2012, Accepted May 31, 2012)*

**Abstract.** This paper focuses on the application of Fuller's ideal gradation curve to theoretically design blended ratio of all solid materials of high performance concrete (HPC), with the aid of error function, and then to study the effect of rice husk ash (RHA) on the performance of HPC. The residual RHA, generated when burning rice husk pellets at temperatures varying from 600 to 800$^{o}$C, was collected at steam boilers in Vietnam. The properties of fresh and hardened concrete are reviewed. It is possible to obtain the RHA concrete with comparable or better properties than those of the specimen without RHA with lower cement consumption. High flowing concrete designed by the proposed method was obtained without bleeding or segregation. The application of the proposed method for HPC can save over 50% of the consumption of cement and limit the use of water. Its strength efficiency of cement in HPC is 1.4-1.9 times higher than that of the traditional method. Local standards of durability were satisfied at the age of 91 days both by concrete resistivity and ultrasonic pulse velocity.

**Keywords:** fuller's ideal gradation curve; high performance concrete; rice husk ash; strength efficiency; durability.

## 1. Introduction

High performance concrete (HPC), as it is well known, can be designed to have the desired higher workability, higher mechanical properties and/or greater resistance to chemical attack than that of traditional concrete (Atcin 1998, Hwang 2003). Many waste materials have been proven to be successfully utilized in the manufacturing of normal concrete and even HPC such as silica fume, fly ash, blast-furnace slag and rice husk ash (RHA). Among those pozzolanic materials, RHA is produced from rice husk which is a waste product from the rice industry. The optimized RHA, by controlled burning and/or grinding, has been used as a pozzolanic material in cement and concrete. The results of its use provide several advantages, such as improved strength and durability properties, and environmental benefits related to the disposal of waste materials and to reduced carbon dioxide emissions (Hwang and Wu 1989, Bui *et al.* 2005, Saraswathy and Song 2007, Sumrerng and Prinya 2008, Zerbino *et al.* 2011). However, there have only been a few attempts to utilize RHA in the production of high-slump flowing concrete such as (Isaia *et al.* 2003, Cordeiro *et al.* 2009, Salas *et al.* 2009, Rodríguez de Sensale 2010, Safiuddin *et al.* 2010). In addition, mix

* Corresponding author, Professor, E-mail: blatuanlx@yahoo.com

design methods by ACI committee (ACI 211.1 1996) are not suitable for proportioning concrete with high workability such as HPC (Kosmatka *et al.* 1995, Su and Miao 2003). This method often ended with a rich mixture that is liable to bleeding and segregation, and also to the volume instability (Hwang 2003, Okamura 1997).

Vietnam is one of the largest exporters of rice in the world, producing large volumes of husk in a three-season year. The Mekong Delta region alone produces 3.6 million tons of rice husks a year. Because of the high energy capacity of rice husk (about 3200 kcal/kg, two barrels of oil by rice husk ton) (Gonçalves and Bergmann 2007, Zerbino *et al.* 2011) a large amount of rice husk has been used as bio fuel to power boilers, producing steam for drying and the parboiling process. In the future, rice husk from the Delta will be used to fuel thermoelectric plants. The rice husk has a large dry volume due to its low bulk density (90-150 kg/m$^3$) (Hwang and Chandra 1996). To save storage space and transport rice husk economically, most rice husk was made into pellets. However, residual RHA, generated when burning rice husk pellets, should be considered for its environmental effects. However, up to now, little research has been done to investigate the use of RHA as supplementary material in cement and concrete production in Vietnam.

According to some concrete research (Kosmatka *et al.* 1995, Neville 1997, Aítcin 1998, Malhotra 2002), reducing water content is the major strategy to reduce bleeding and segregation, and to improve the volume stability. Therefore, in Taiwan, the Hwang's research group used the Densified Mixture Design Algorithm (DMDA) to achieve the maximum dry loose density by simply packing all solid particles including coarse aggregate, sand and fly ash, to reduce the quantity of lubricating paste but keep the desired workability for HPC. This method has been successfully applied to many projects in Taiwan (Hwang *et al.* 2001, Tsai *et al.* 2009), including its use in the construction of Taipei 101, one of the world's tallest buildings (Chen *et al.* 1995, Lee and Hwang 2002). The major difference from other mixture design algorithms is that instead of partial replacement of cement, DMDA incorporating pozzolanic material is used to fill the void of aggregates and hence increase the density of the aggregate system. The purpose of such action is to reduce the cement paste content for design properties such as workability, strength and durability. As a result, both the pozzolanic effect and the physical or filler effect can be obtained. As the category of material is less than three, the blend ratio ($\alpha$, $\beta$) (Hwang and Chen 2002, Lee and Hwang 2002) of solid materials can be easily obtained by experimental work; otherwise the packing seems difficult, especially as the material size is finer than $\mu$m. Therefore, it is necessary to adopt a numerical approach to obtain a proper packing order of all the granular materials.

The Fuller gradation curve, on which the densification theory is based, has been successfully applied to asphalt concrete; for concrete it has been applied to blended coarse and fine aggregates but has not been effectively applied to ultrafine particles as well as the particle category more than three (Mora *et al.* 1998). From this point, the Hwang's research group has researched combining the theoretical Fuller's ideal gradation curve with DMDA to propose a mix design method (let HFDMDA as notation of the proposed method). In HFDMDA method, the Fuller's Curve is applied to enable full packing with all solid particles such as sand, pozzolans and cement in size ranging from mm, $\mu$m to nm. To simplify the derivation, it is necessary to assume that the aggregate be spherical, which is definitely different from reality and thus will give rise to some errors. Therefore, least square method is applied to minimize the derivation. After determining solid particle ratio, the water content can be calculated based on the assigned amount of lubricated paste and quality of HPC.

In order to test the likely practicality of the HFDMDA method, HPC mixtures will be designed by this proposed method in this investigation. Residual RHA that is generated when burning rice husk pellets is used as a supplementary cementitious material. For comparison purposes, HPC mixtures are also calculated by ACI 211.1 (ACI 211.1 1996). Two kinds of concrete are investigated in terms of the compressive strength and durability as well as strength efficiency of cement.

## 2. Mixture design procedures of the proposed method

The HFDMDA method is based upon the theoretic structure of densified mix design and is combined with Fuller's grading curve (Fuller and Thompson 1906) to simplify the process of concrete mix design by using a calculation of derivation of each process and finally to optimize the mixture proportion of concrete. The procedures of HFDMDA method can be summarized in the following steps:

### *2.1 Step 1*

Select the maximum diameter of aggregate ($D_{\max}$) to calculate the volume portion of each material on a designated sieve from the ideal gradation curve (Fuller's curve) according to Eq. (1).

$$P = 100\left(\frac{d}{D}\right)^{h} \quad h = \frac{1}{3} \sim \frac{1}{2} \tag{1}$$

### *2.2 Step 2*

Mix the aggregate gradation with the theoretical Fuller's ideal curve grading data and substitute into the following formula (Eq. (2)) to estimate the aggregate proportion of under $h$-th power of Fuller's gradation curve.

$$[Pv]_{n-1} = [([A]_{i,j}^{T} - [1]_{n-1\times1}[A]_{n,j}^{T})([A]_{i,j} - [A]_{n,j}[1]_{n-1\times1}^{T})]^{-1} \times ([A]_{i,j}^{T} - [1]_{n-1\times1}[A]_{n,j}^{T})([k]_{m} - [A]_{n,j}) \tag{2}$$

The Eq. (2) is calculated by the least square method (Eq. 3) from the discrete quantity of gradation curves of blended aggregate and the theoretical Fuller's ideal gradation curve.

$$M = R^2 = \sum_{j=1}^{m}\left(\sum_{i=1}^{n} Pv_i a_{i,j} - k_j\right)^2 \tag{3}$$

where $M$ is the discrete amount; $R$ is the error of the actual passing of $i$-material.

After that, the optimal blended ratio $Pv_1$: $Pv_2$...: $Pv_n$ (Example: $Pv_{ca}$: $Pv_{cs}$: $Pv_{RHA}$) can then be calculated.

### *2.3 Step 3*

To convert the volume ratio ($Pv_i$) of blended aggregate to weight ratio ($Pw_i$) under $h$-th power of the Fuller's ideal gradation curve and measure dry loose density and packing volume ratio of the blended aggregate. The experiment is conducted to obtain the dry loose density ($U_{\max}$) of blended aggregate according to the hand-dry roding method in accordance with the ASTM C29 standard.

### 2.4 Step 4

To decide the best aggregate structure under power law ($h$).

Choosing power law ($h$) depends on the approach to the ideal grading curve, the maximum packing curve, the maximum unit weight and other factors such as: workability, effective cost, blended aggregate ratio and trial batch results.

### 2.5 Step 5

To estimate the coating thickness of lubricating paste ($t$) on the surface of the total blended aggregate ($S$) in total paste amount needed ($V_p(V_p = V_v + S \times t)$) and calculate the volume of void ($V_v$) within the aggregate under dense packing state by Eq. (4).

$$V_v = 1 - U_{\max} \times \left(\frac{Pw_1}{\gamma_1} + \frac{Pw_2}{\gamma_2}\right) \tag{4}$$

Here: $Pw_1$: Weight percentage of coarse aggregate portion of blended aggregate; $Pw_2$: Weight percentage of fine aggregate portion of blended aggregate; $\gamma_1$, $\gamma_2$: Specific gravity of coarse aggregate and fine aggregates, respectively.

### 2.6 Step 6

To calculate total surface area of the blended aggregate by statistics under the assumption that the aggregate particle is spherical.

This calculation requires the above-mentioned aggregate grading data, which uses

$$Kss,_j = \frac{6}{(\ln d_{i,j+1} - \ln d_{i,j})}\left(\frac{1}{d_{i,j}} - \frac{1}{d_{i,j+1}}\right)$$

to get the surface area of each individual aggregate size ranging between $d_{i,j+1}$ and $d_{i,j}$. Hence the entire surface area of blended aggregates per unit mass ($Ksst$) can be calculated by using Eq. (5).

$$Ksst = \sum_{j=1}^{10}\left[\left(\frac{Pw_1}{\gamma_1}a_{1,j} + \frac{Pw_2}{\gamma_2}a_{2,j}\right)Kss,_j\right] \tag{5}$$

### 2.7 Step 7

To calculate the content of each constituent material of concrete. List the formulas of material relation function, build up a relation matrix and finally obtain the materials proportion of concrete by inversing the matrix.

In this study, HPC mainly consists of five materials, such as fine aggregate ($w_{cs}$), coarse aggregate ($w_{ca}$), cement ($w_c$), RHA ($w_{RHA}$) and water ($w_w$). To solve the blended ratios of ingredient materials, five condition equations can be enumerated according to relations, and the amount of each material can be derived via matrix analysis by the procedure below:

The total surface of the blended aggregate: $S = U \times Ksst$

The total paste amount needed:

$$V_p = V_v + S \cdot t = V_v + U \cdot Ksst \cdot t = V_v + (w_{ca} + w_{cs}) \cdot Ksst \cdot t \tag{6}$$

It is known that "cement past" is composed of "cement, RHA and water". Eq. (6) can be transposed to Eq. (7).

$$Ksst\cdot t\cdot w_{ca}+Ksst\cdot t\cdot w_{cs}-\frac{w_{RHA}}{\gamma_{RHA}}-\frac{w_c}{\gamma_c}-\frac{w_w}{\gamma_w}=-V_v \tag{7}$$

Total volume of coarse aggregate and fine aggregate

$$\left(Ksst\cdot t+\frac{1}{\gamma_{ca}}\right)w_{ca}+\left(Ksst\cdot t+\frac{1}{\gamma_{cs}}\right)w_{cs}=1-V_a-V_v=1-V_a-V_v-(w_{ca}+w_{cs})\cdot Ksst\cdot t \tag{8}$$

$$\frac{w_{ca}}{Pw_1}=\frac{w_{cs}}{Pw_2}=\frac{w_{RHA}}{Pw_3} \tag{9}$$

Eq. (9) can be revised into Eqs. (10) and (11).

$$w_{ca}-\frac{Pw_1}{Pw_2}w_{cs}=0 \tag{10}$$

$$w_{ca}-\frac{Pw_1}{Pw_3}w_{RHA}=0 \tag{11}$$

$\frac{w}{b}=\frac{w_w}{w_c+w_{RHA}}$ ratio can be converted into: $\left(\frac{w}{b}\right)\cdot w_{RHA}+\left(\frac{w}{b}\right)\cdot w_c-w_w=0$ (12)

Five conditional Eqs: (7), (8), (10), (11) and (12) can be rewritten as Eq. (13)

$$\begin{bmatrix} Ksst\cdot t & Ksst\cdot t & -\frac{1}{\gamma_{RHA}} & -\frac{1}{\gamma_c} & -\frac{1}{\gamma_w} \\ Ksst\cdot t+\frac{1}{\gamma_{ca}} & Ksst\cdot t+\frac{1}{\gamma_{cs}} & 0 & 0 & 0 \\ 1 & -\frac{Pw_1}{Pw_2} & 0 & 0 & 0 \\ 1 & 0 & -\frac{Pw_1}{Pw_3} & 0 & 0 \\ 0 & 0 & w/b & w/b & -1 \end{bmatrix}\begin{bmatrix} w_{ca} \\ w_{cs} \\ w_{RHA} \\ w_c \\ w_w \end{bmatrix}=\begin{bmatrix} -V_v \\ 1-V_a-V_v \\ 0 \\ 0 \\ 0 \end{bmatrix} \tag{13}$$

Content of each material can be calculated from Eq. (14)

$$\begin{bmatrix} w_{ca} \\ w_{cs} \\ w_{RHA} \\ w_c \\ w_w \end{bmatrix}=\begin{bmatrix} Ksst\cdot t & Ksst\cdot t & -\frac{1}{\gamma_{RHA}} & -\frac{1}{\gamma_c} & -\frac{1}{\gamma_w} \\ Ksst\cdot t+\frac{1}{\gamma_{ca}} & Ksst\cdot t+\frac{1}{\gamma_{cs}} & 0 & 0 & 0 \\ 1 & -\frac{Pw_1}{Pw_2} & 0 & 0 & 0 \\ 1 & 0 & -\frac{Pw_1}{Pw_3} & 0 & 0 \\ 0 & 0 & w/b & w/b & -1 \end{bmatrix}^{-1}\begin{bmatrix} -V_v \\ 1-V_a-V_v \\ 0 \\ 0 \\ 0 \end{bmatrix} \tag{14}$$

### 2.8 The feature of mixture design

In the HFDMDA method, the particle distribution of the mixture material covers mm, $\mu$m to nm, so that materials can be fit together to form the most dense state. By the estimation of surface area of particle and the pore (void), the assumption of the designate coating thickness on the surface of the aggregate and the paste content based on the requirement of design strength and the target concrete quality can be controlled. The mixed proportion of less water, less cement and more aggregate proposed/ discovered by the HFDMDA may be suggested to be the selection for design properties such as volume stability, workability, strength and durability.

The power $h$ values suggested are about 1/2-1/3 in Fuller curve $P=(d/D)^h$. The larger the $h$ power, the more the coarse aggregate. On the contrary, the smaller the $h$ power, the more the fine aggregate. The optimum $h$ for concrete is about 1/2 (Hwang 2003, Fuller and Thompson 1906). The selection of the materials for Fuller's curve dense packing suggested that the particle distribution shall not be too close; otherwise the calculation may produce the "crowding - out phenomenon".

## 3. Sample calculation of the proposed method

The Type I Portland cement was produced by Taiwan Cement Company. Crushed coarse aggregate and natural sand were provided by local quarries. The mixing water was local tap water. Type-G superplasticizer, having 43% solid content with specific gravity of 1.18, was used to achieve the desired workability for all concrete mixtures. All materials conform to the related ASTM standards and their physical properties as well as chemical compositions are shown in Table 1. The maximum size of coarse aggregates ($D_{max}$) is 19 mm and specific gravity of coarse aggregates ($\gamma_{ca}$) is 2.67. The specific gravity of fine aggregate ($\gamma_{cs}$) is 2.65. The specific gravity of cement ($\gamma_c$) is 3.15, specific gravity of RHA ($\gamma_{RHA}$) and water ($\gamma_w$) are 2.06 and 1, respectively.

### 3.1 Step 1

The maximum diameter of coarse aggregate ($D_{max}$) is 19 mm. The volume portion of each

Table 1 Physical and chemical analysis of cement and RHA

| | Item | Cement | RHA |
|---|---|---|---|
| Physical properties | Specific gravity | 3.15 | 2.06 |
| | Mean particle size ($\mu$m) | 16 | 12 |
| Chemical compositions (%) | $SiO_2$ | 22.01 | 91 |
| | $Al_2O_3$ | 5.51 | 0.35 |
| | $Fe_2O_3$ | 3.44 | 0.41 |
| | MgO | 2.59 | 0.81 |
| | $SO_3$ | 2.03 | 1.21 |
| | $P_2O_5$ | 0.05 | 0.98 |
| | $Na_2O$ | 0.40 | 0.08 |
| | $K_2O$ | 0.70 | 3.21 |
| | Loss on ignition (%) | 0.51 | 8.5 |

Table 2 Sieve analysis results of coarse aggregate, fine aggregate and RHA

| Sieve number | < #100 | #100 | #50 | #30 | #16 | #8 | #4 | 3/8" | 1/2" | 3/4" |
|---|---|---|---|---|---|---|---|---|---|---|
| Sieve size $d_{i,j}$ (mm) | - | 0.15 | 0.30 | 0.60 | 1.18 | 2.36 | 4.75 | 9.5 | 12.5 | 19.0 |
| *Kss,j* (1/mm) | 0 | 28.85* | 14.43 | 7.27 | 3.67 | 1.83 | 0.91 | 0.55 | 0.39 | 0.28 |
| Amount passing (%) (Fuller's curve) | 0 | 8.89** | 12.57 | 17.77 | 24.92 | 35.24 | 50.00 | 70.71 | 81.11 | 100 |
| Amount retained, $k_j$ (%) (Fuller's curve) | 8.89 | 3.68 | 5.20 | 7.15 | 10.32 | 14.76 | 20.71 | 10.40 | 18.89 | 14.71 |
| Amount retained (%) (Coarse aggregate) | 0.7 | 0 | 0 | 0 | 0 | 0 | 36.1 | 41.4 | 21.8 | 0 |
| Amount retained (%) (Fine aggregate) | 4.8 | 9.5 | 13.6 | 15.5 | 27.7 | 29 | 0 | 0 | 0 | 0 |
| Amount retained (%) (Rice husk ash) | 1 | 0 | 0 | 0 | 0 | 0 | 0 | 0 | 0 | 0 |

Remark: $^{*}Kss_j = \frac{6}{(\ln d_{j+1} - \ln d_j)}\left(\frac{1}{d_j} - \frac{1}{d_{j+1}}\right) = \left(\frac{6}{\ln 0.3 - \ln 0.15}\right)\left(\frac{1}{0.15} - \frac{1}{0.30}\right) = 28.85(1/\text{mm})$

$^{**}$Amount passing (%) : $P = 100\left(\frac{d}{D}\right)^h = 100\left(\frac{d}{D_{\max}}\right)^{0.5} = 100\left(\frac{0.15}{19}\right)^{0.5} = 8.89\%$

material on a designated sieve from the ideal gradation curve (Fuller's curve) according to Eq. (1) can be calculated as shown in Table 2. The power $h$ value of 0.5 was chosen.

### 3.2 Step 2

Based on the data from Table 2, $[A]_{i,j}$, $[A]_{n,j}$, $[k]_m$, $[1]_{n-1\times 1}$, $[P]_{n-1}$ and $[Kss_j]$ matrices can be defined as below:

Substitute $[A]_{i,j}$, $[A]_{n,j}$, $[k]_m$, $[1]_{n-1\times 1}$ matrices into Eq. (2), then the optimal blended ratio $P_{v1}$: $P_{v2}$: $P_{v3}$ can be calculated:

$P_{v1(coarse\ aggregate)} = 0.4700$; $P_{v2(fine\ aggregate)} = 0.4614$; $P_{v3(RHA)} = 0.0686$

$$[A]_{i,j} = \begin{bmatrix} 0.007 & 0.048 \\ 0 & 0.095 \\ 0 & 0.136 \\ 0 & 0.155 \\ 0 & 0.277 \\ 0 & 0.290 \\ 0.361 & 0 \\ 0.414 & 0 \\ 0.218 & 0 \\ 0 & 0 \end{bmatrix}; \ [A]_{n,j} = \begin{bmatrix} 1 \\ 0 \\ 0 \\ 0 \\ 0 \\ 0 \\ 0 \\ 0 \\ 0 \\ 0 \end{bmatrix}; \ [k]_m = \begin{bmatrix} 0.0889 \\ 0.0368 \\ 0.0520 \\ 0.0715 \\ 0.1032 \\ 0.1476 \\ 0.2071 \\ 0.1040 \\ 0.1889 \\ 0.1471 \end{bmatrix}; \ [Kss_j] = \begin{bmatrix} 0 \\ 28.85 \\ 14.43 \\ 7.27 \\ 3.67 \\ 1.83 \\ 0.91 \\ 0.55 \\ 0.39 \\ 0.28 \end{bmatrix}; \ [1]_{n-1\times n} = \begin{bmatrix} 1 \\ 1 \end{bmatrix} \ [P_v]_{n-1} = \begin{bmatrix} P_{v1} \\ P_{v2} \end{bmatrix}$$

### 3.3 Step 3

The volume ratio ($Pv_i$) of blended aggregate was converted to weight ratio ($Pw_i$)

$$P_{w1}=0.4792;\ P_{w2}=0.4668;\ P_{w3}=0.0540$$

Based on $P_{w1}$: $P_{w2}$: $P_{w3}$ ratio, using the hand-dry roding method in accordance with the ASTM C29 standard, one gets the dry loose density of blended aggregate: $U_{\max} = 2046\ \text{kg/m}^3$.

### 3.4 Step 4

The power $h$ value of 0.5 was chosen in this example.

### 3.5 Step 5

Coating thickness of lubricating paste ($t$) was estimated by 5 $\mu$m. Volume of void ($V_v$) within the aggregate under dense packing state can be calculated based on the Eq. (4).

$$V_v = 1+-U_{\max}\left(\frac{P_{w1}}{\gamma_{ca}}+\frac{P_{w2}}{\gamma_{cs}}\right) = 1-2046\left(\frac{0.4792}{2670}+\frac{0.4668}{2650}\right) = 0.2724\ \text{m}^3$$

### 3.6 Step 6

The entire surface area of blended aggregate per unit mass ($Ksst$) can be calculated by using Eq. (5)

$$Ksst = \sum_{j=1}^{10}\left[\left(\frac{P_{w1}}{\gamma_{ca}}a_{1,j}+\frac{P_{w2}}{\gamma_{cs}}a_{2,j}\right)Kss_j\right] = \sum_{j=1}^{10}\left[\left(\frac{0.4792}{2670}a_{1,j}+\frac{0.4668}{2650}a_{2,j}\right)Kss_j\right] = 1.4148\ (\text{m}^2/\text{kg})$$

### 3.7 Step 7

Air content $V_a = 2\%$ and $w/b = 0.35$ were used in this example.

Substitute the needed values into the Eq. (14), amount of materials needed per unit volume of concrete can be obtained.

$$\begin{bmatrix} w_{ca} \\ w_{cs} \\ w_{RHA} \\ w_c \\ w_w \end{bmatrix} = \begin{bmatrix} 7.074\times10^{-6} & 7.074\times10^{-6} & -\frac{1}{2060} & -\frac{1}{3150} & -\frac{1}{1000} \\ 7.074\times10^{-6}+\frac{1}{2670} & 7.074\times10^{-6}+\frac{1}{2650} & 0 & 0 & 0 \\ 1 & -\frac{0.4792}{0.4668} & 0 & 0 & 0 \\ 1 & 0 & -\frac{0.4792}{0.0540} & 0 & 0 \\ 0 & 0 & 0.35 & 0.35 & -1 \end{bmatrix}^{-1} \begin{bmatrix} -0.2724 \\ 0.7076 \\ 0 \\ 0 \\ 0 \end{bmatrix}$$

Solve the above equation, the content of each material can obtain: Coarse aggregate: $w_{ca}$=936 kg/m$^3$; Fine aggregate: $w_{cs}$=912 kg/m$^3$; Cement: $w_c$=296 kg/m$^3$; Rice husk ash: $w_{RHA}$=105 kg/m$^3$; Water: $w_w$=140 kg/m$^3$.

## 4. Material and experimental methods

### 4.1 RHA characteristics

The residual RHA was collected at Saigon Ve Wong Co., Ltd., Ho Chi Minh city, Vietnam. Rice husk pellets were burnt in a steam boiler at temperatures varying from 600 to 800°C. X-ray power diffraction results of RHA show that RHA is mostly amorphous silica and partially crystalline silica. The SEM results show that RHA has a porous cellular structure and consists of irregular-shaped particles. To increase the finesses, the residual RHA was ground by a ball mill for 1 h. By this way, the average particle size of RHA can be decreased to 12 $\mu$m in diameter, as was measured using Mastersizer 2000. The chemical composition of RHA was presented in Table 1. High value of silica content and loss on ignition (presented the amount of residual carbon) can be observed.

### 4.2 Testing program

The mixture proportions designed by HFDMDA and ACI 211.1 are listed in Table 3. The concrete mixtures in this investigation were calculated with the same water-to-binder ratio of 0.35. For ACI method, the mixtures were prepared by replacing 0%, 10%, 20% and 30% of weight of cement with RHA. Three coating paste thicknesses ($t$): 5 $\mu$m, 15 $\mu$m and 25 $\mu$m were investigated for HFDMDA method.

The compressive strength, concrete resistivity and ultrasonic pulse velocity were conducted according to the relevant ASTM standards. Slump and slump flow spread of HPC specimens were controlled to meet the HPC requirement which is 230-270 mm and 500-700 mm, respectively. The strength efficiency of cement in each HPC was also calculated in this study.

Table 3 Mixture proportion of HPC

| Mix no. | $w/b$ | $w/c$ | RHA (%) | Coating thickness ($\mu$m) | Mix proportion (kg/m$^3$) | | | | |
|---|---|---|---|---|---|---|---|---|---|
| | | | | | Coarse aggregate | Sand | Cement | RHA | Water+SP |
| A35-00 | 0.35 | 0.35 | 0 | - | 933 | 633 | 571 | 0 | 200 |
| A35-10 | 0.35 | 0.39 | 10 | - | 933 | 608 | 514 | 57 | 200 |
| A35-20 | 0.35 | 0.44 | 20 | - | 933 | 582 | 457 | 114 | 200 |
| A35-30 | 0.35 | 0.50 | 30 | - | 933 | 557 | 400 | 171 | 200 |
| F35-05 | 0.35 | 0.47 | 26 | 5 | 936 | 912 | 296 | 105 | 140 |
| F35-15 | 0.35 | 0.46 | 23 | 15 | 903 | 879 | 337 | 102 | 154 |
| F35-25 | 0.35 | 0.44 | 21 | 25 | 871 | 849 | 376 | 98 | 166 |

Remark: Mix no: "A" represents the ACI 211.1 method, Mix no: "F" presents the HFDMDA method practice for selecting proportion for concrete.

Table 4 Fresh properties of HPC

| Mix no. | *w/b* | *w/c* | Slump (mm) | Slump flow (mm) | Flow time (s) |
|---|---|---|---|---|---|
| A35-00 | 0.35 | 0.35 | 240 | 560 | 16 |
| A35-10 | 0.35 | 0.39 | 240 | 510 | 27 |
| A35-20 | 0.35 | 0.44 | 250 | 610 | 49 |
| A35-30 | 0.35 | 0.50 | 230 | 500 | 19 |
| F35-05 | 0.35 | 0.47 | 230 | 535 | 20 |
| F35-15 | 0.35 | 0.46 | 245 | 500 | 22 |
| F35-25 | 0.35 | 0.44 | 245 | 530 | 29 |

## 5. Results and discussions

### 5.1 Slump and slump flow spread

The fresh properties of HPC specimens are shown in Table 4. The water content has a great influence on the flowage of concrete. Too much water results in a higher possibility of bleeding and segregation, which is not favorable for strength development, interface bond strength, volumetric stability and durability (Mindess S 1981, Aítcin 1998, Hwang *et al.* 2001, Hwang 2003).

The results indicate that good workability was too difficult to obtain in HPC specimens designed by ACI 211.1. This is due to high water content in concrete. High-slump flowing concrete (slump > 230 mm) designed by HFDMDA was obtained without bleeding or segregation. The results may be due to the fact that there is less void content within aggregate and less paste is required for the same workability. A comparison of the two results reveals that the amount of water used is employed as a criterion by the ACI. The water to cement ratio has a direct influence on the cement content. Generally speaking, a low water to cement ratio represents a high paste content indicating high strength. As a result, the amount of water has often been wrongly employed as an index for controlling the slump and workability of concrete. In fact, for HPC to achieve high workability, it has to be most densely packed with least voids. This can be achieved by controlling the gradation of aggregate. In addition, it requires the use of sufficient amount of paste, along with pozzolanic materials and superplasticizers.

### 5.2 Compressive strength

Compressive strength is usually considered to be one of the most important properties of concrete and a major indicator of general quality control. Fig. 1(a) shows the relationship between testing age and the compressive strength of concrete with various RHA contents at the same *w/b* ratio. In the early phase, the addition of RHA reduces the amount of cement by 10-20%, the volume of capillary pores then increases, accumulating CH on the interface. As a result, the structure is less compact, causing the strength to be lower than that of the specimen without RHA added. The pozzolanic reaction process increases along with curing time, which will decrease the amount of CH and improve the densification (Zhang *et al.* 1996). Consequently, the compressive strength is enhanced in the later phase. Comparison of the data for 91 days of testing ages shows that the compressive

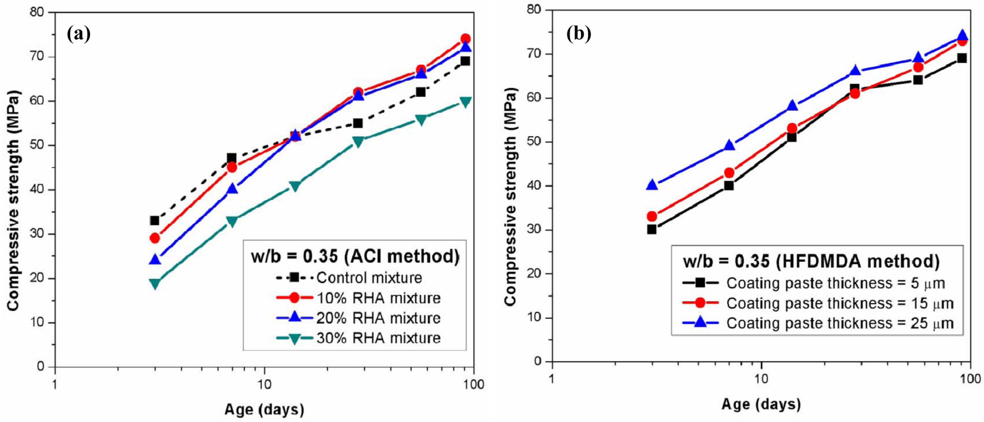


Fig. 1 The strength development of HPCs designed by ACI 211.1 (a) and HFDMDA (b) methods

strength of concretes with up to 20% replacement of RHA attain values equivalent to that control concrete specimens.

Fig. 1(b) shows the development of compressive strength of HPC with three coating paste thickness values. In the early age, the concrete with high cement paste content and low *w/c* will develop high strength as expected. But at later age, concrete with low paste content will gradually develop compressive strength through the pozzolanic reaction of RHA with cement from hydration of cement. The addition of pozzolanic materials as filler of aggregate in concrete is physically not only helpful to promote the packing density of aggregate but also chemically improves the interface transition zone properties through pozzolanic reaction. This reaction converts at least 20% of calcium hydroxide of cement paste to form low density C-S-H gel that will contribute to long-term performance of concrete. Therefore, after 91-day age the compressive strength of the HPC with all levels of paste content is equivalent.

In comparison, not including the concrete with 30% RHA replacement (mixture A35-30 as shown in Table 3), the results indicate that the compressive strength of the concrete designed by ACI 211.1 and HFDMDA is equivalent at the age of 91 days. On the other hand, to obtain HPC with 60-62 MPa compressive strength range at 28 days, the consumption of cement required by HFDMDA method is only 296-337 kg/m$^3$, while that of ACI method is 514-457 kg/m$^3$ (as shown in A35-10, A35-20, F35-05 and F35-15 concrete mixtures). Thus, the application of the proposed method for HPC can save over 50% of the consumption of cement.

### *5.3 Strength efficiency of cement*

The strength efficiency of cement implies the yielded strength per kilogram of cement denoted as MPa/kg cement. Fig. 2(a) shows the strength efficiency of cement with different RHA contents by ACI 211.1. The 91-day strength efficiency of cement rises to 0.14, 0.16 and 0.15 MPa/kg/m$^3$ corresponding to the RHA concrete with percentage replacement of the ash of 10%, 20% and 30%, respectively. The 91-day value is 1.2-1.3 times higher than that of the control concrete (0.12 MPa/kg/m$^3$).

Fig. 2(b) shows that the 91-day strength efficiency of cement rises to 0.23, 0.22 and 0.20 MPa/kg/m$^3$ corresponding to the RHA concrete with the coating thickness paste value of 5, 15 and 25 $\mu$m,

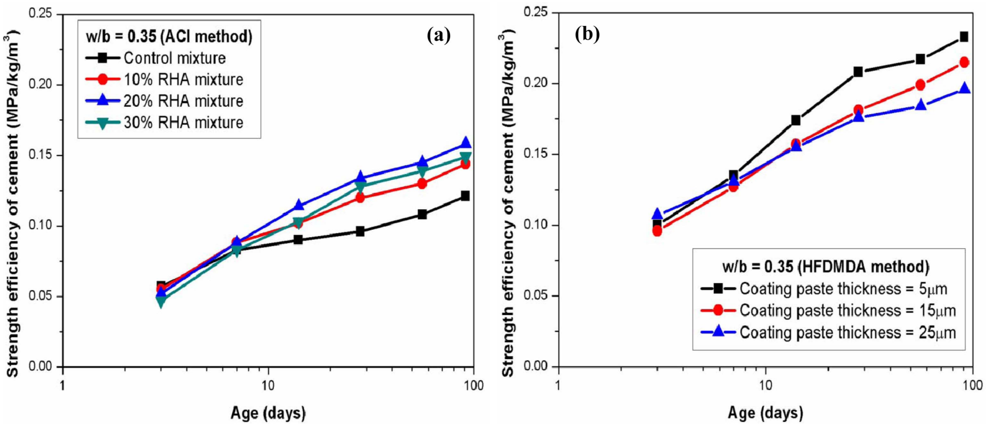


Fig. 2 The strength efficiency of cement of HPCs designed by ACI 211.1 (a) and HFDMDA (b) methods

respectively. Comparing with the strength efficiency between 0.14 and 0.16 MPa/kg/m$^3$ of cement achieved by ACI 211.1, we conclude that the application of RHA for void filling and densifying the concrete structure does consume calcium hydroxide to form low-density C-S-H gel, thus improving concrete strength. Therefore, even high *w/c* ratio, high RHA content, low amount of water (low amount of paste) may affect early compressive strength, but the strength efficiency of cement still attains better value. The strength efficiency of cement for HPC designed by HFDMDA method is 1.4-1.9 times higher than that of the traditional one in comparison at the same strength. Thus, the cement consumption, the energy consumption, and the detrimental $CO_2$ emission for the environment during the production of cement can be significantly reduced. Also, the concrete problems due to large cement content, such as thermal cracking, abnormal expansion, chemical degradation, etc. can be minimized and the service life of concrete structures could be lengthened (Mindess S 1981, Mehta 1986, Hwang 2003).

### *5.4 Electrical resistance*

The measurement of concrete electrical resistivity gives an indication of durability of concrete. The conduction of ions of the hydration solution in the pores causes corrosion. According Hope *et al.* (Hope *et al.* 1985), the minimum value beyond which corrosion cannot occur is 8.5 kΩ/cm, while Buenfeld *et al.* (Buenfeld *et al.* 1986) recommended the value is 20 kΩ/cm, which corresponds to the special specification of HPC. The higher the electrical resistance, the greater the corrosion endurance will be. In this study, the pozzolanic reaction due to the addition of RHA reduces the volume of capillary pores and enhances the impermeability of concrete. The electrical resistance will grow with the concrete age through pozzolanic reaction of RHA. Therefore, its pozzolanic reaction is not expected to be significant in early age and the electrical resistance is low. As seen in Fig. 3(a), after 28 days, the electrical resistance of the concretes with RHA added rises sharply. This indicates the effects of solidification brought by pozzolanic reaction, which can indeed increase the electrical resistance of concrete.

For the aforesaid test, the electrical resistance of concrete is related to the density of concrete and especially to the amount of water (Hope *et al.* 1985, Buenfeld *et al.* 1986, Hwang 2003). The concrete designed by HFDMDA with the same *w/b* ratio, the lower the coating paste thickness, the

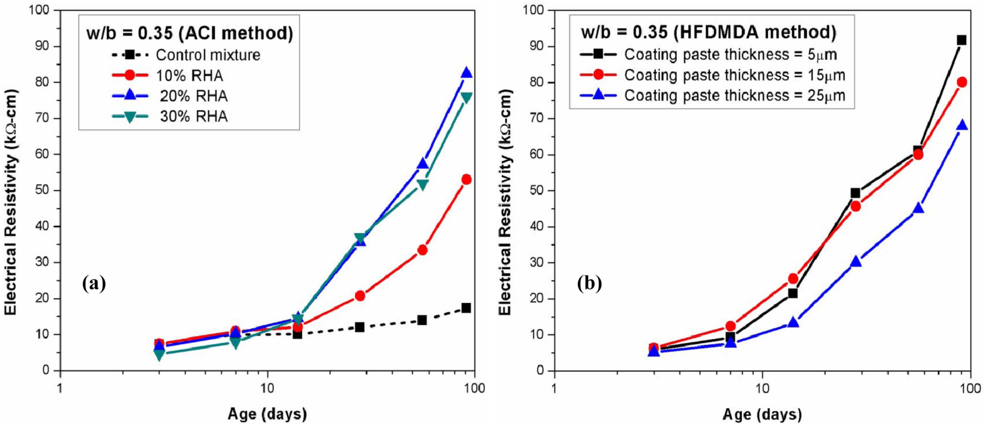


Fig. 3 The development of electrical resistivity of HPCs designed by ACI 211.1 (a) and HFDMDA (b) methods

higher the concrete resistivity. For examples, F3505 reaches 91.8 kΩ-cm (Fig. 3(b)), and F3525 reaches 67.9 kΩ-cm. This is due to the less the water content, the less the macro-pores in concrete, and the less the conductivity of the concrete is. The electrical resistance will grow with the concrete age through pozzolanic reaction. After 28 days, resistivity of both the concrete added RHA designed by HFDMDA and by ACI is higher than 20 kΩ-cm, therefore, the specimens might be considered to be durable concrete (Buenfeld *et al.* 1986).

### *5.5 Ultrasonic pulse velocity (UPV)*

The pulse velocity methods have been used to assess the uniformity and relative quality of concrete, to indicate the presence of voids and cracks, and to evaluate the effectiveness of crack repairs (ASTM C597 2002). Generally, high pulse velocity reading in concrete is indicative of concrete of good quality. Malhotra (Malhotra 1976) has suggested that concrete has good durability when its pulse velocity value is in the range of 3660-4575 m/s.

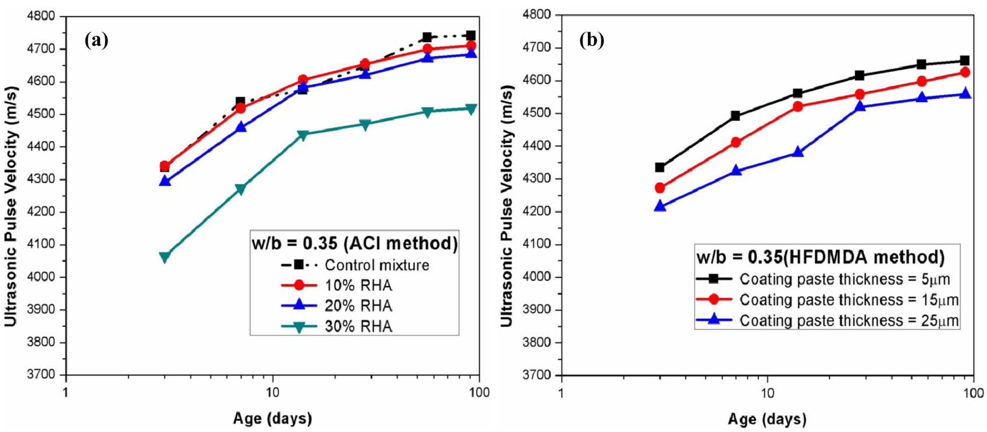


Fig. 4 The development of UPV of HPCs designed by ACI 211.1 (a) and HFDMDA (b) methods

Fig. 4(a) shows that the effect of RHA content on UPV in concrete is to cure with age. An increase in RHA content tends to lower the UPV curve. In the long run, the addition of RHA up to 20% will finally reach the same UPV values as in the control concrete. Measurement shows that UPV continues to grow when less cement is used. If more cement is used, the UPV will decrease (Hwang *et al.* 2001). Such an occurrence may be explained by the fact that the control concrete contains greater quantities of cement than RHA cement paste does and has higher hydrate content at the same age. Due to the much more porous structure and lower specific gravity of RHA particles compared to cement, the grains of RHA are not as dense as those of cement. However, at 28 days, UPV of all specimens is higher than 3660 m/s, therefore, the specimens might be considered to be durable concrete (Malhotra 1976).

Fig. 4(b) indicates the development of UPV with various coating paste thickness values of concrete designed by HFDMDA, and it clearly shows that the lower the cement paste content is, the higher the UPV of concrete will be. Previous research points out the sequence of UPV of each ingredient of normal weight concrete is coarse aggregate > sand > paste (Hwang and Chen 1998). Therefore, concrete with low cement paste content is mainly occupied by aggregates and consequently has high UPV. It also implies that high paste content will encounter the risk of micro-crack in the paste system that is harmful to the durability of HPC.

## 6. Conclusions

1. When compared, control concrete without added ashes and concrete replacing up to 20% of cement by RHA achieved similar compressive strength and durability properties. The strength efficiency of cement in RHA blended concrete is much higher than that of the control concrete. It indicates a possible use of the RHA as a partial Portland cement substitute. Moreover, while the results will be able to substantiate the viability of application of RHA in concrete industry under the prevailing conditions in Vietnam, they are also expected to be especially useful for future studies on RHA in a specific condition in this country.
2. In general, the higher cement paste content is, the higher compressive strength will be. In the study, the concrete with high coating thickness (high cement paste content) will develop high strength as expected in the early age. However, after 91-day age the compressive strength of HPC with all levels of paste content is equivalent. This is due to the slow pozzolanic reaction of RHA.
3. The technique of HFDMDA overcomes concrete problems through aggregate gradation, and minimizes the paste content. Therefore, as the results, the HPC designed by HFDMDA does have high performance with high flow ability without bleeding or segregation, cost-effectiveness and durable features like HPC after all.
4. By comparison in the same compressive strength range, the advantage of using HFDMDA methods for HPC is to save over 50% in the consumption of cement. The strength efficiency of cement for HPC designed by HFDMDA is 1.4-1.9 times higher than that of the traditional one in comparison.

The application of Fullers ideal grading curve combined with the densified mixture design algorithm for mixture design is more efficient than the conventional mixture design method and the application of the densified mixture design algorithm in laboratory. Therefore, under Fuller's ideal grading curve and error function, the quantitative approach may be introduced into concrete science especially for composite material with efficiency.

## Acknowledgements

The authors thank the Ve Wong Corporation for RHA and the financial support that made this publication possible. We are grateful to Professor Lee-Kuo Lin, Professor Ta-Wui Cheng and other fellows of Hwang's research group for their assistance on this subject to help finish this research.

## References

ACI 211.1 (1996), *Standard practice for selecting proportions for normal, heavyweight, and mass concrete*, ACI Manual of Concrete Practice.

Atcin, P. (1998), *High-performance concrete*, E. & F.N. Spon.

ASTM C597 (2002), *Standard test method for pulse velocity through concrete*, Annual Book of ASTM Standard 04.

Buenfeld, N.R., Newman, J.B. and Page, C.L. (1986), "The resistivity of mortars immersed in sea-water", *Cement Concrete Res*., **16**(4), 511-524.

Bui, D.D., Hu, J. and Stroeven, P. (2005), "Particle size effect on the strength of rice husk ash blended gap-graded Portland cement concrete", *Cement Concrete Comp*., **27**(3), 357-366.

Chen, J.C., Hwang, C.L. and Tsai, D.H. (1995), "Research and development of high performance concrete in Taiwan", *Concrete Int*., **17**(10), 1-76.

Cordeiro, G., Toledo Filho, R. and de Moraes Rego Fairbairn, E. (2009), "Use of ultrafine rice husk ash with high-carbon content as pozzolan in high performance concrete", *Mater. Struct*., **42**(7), 983-992.

Fuller, W.B. and Thompson, S.E. (1906), "The Laws of proportioning concrete", *Trans. ASCE*., **LVII**(2), 67-143.

Gonçalves, M.R.F. and Bergmann, C.P. (2007), "Thermal insulators made with rice husk ashes: Production and correlation between properties and microstructure", *Constr. Build Mater*., **21**(12), 2059-2065.

Hope, B.B., Ip, A.K. and Manning, D.G. (1985), "Corrosion and electrical impedance in concrete", *Cement Concrete Res*., **15**(3), 525-534.

Hwang, C.L., Chang, P.K. and Peng, Y.N. (2001), "Application of high-performance concrete to high-rise building in Taiwan", *Adv. Struct. Eng*., **4**(2), 65-73.

Hwang, C.L. (2003), *The theory and practice of high peformance concrete*, Janes' Book Publisher Co., Taipei, Taiwan.

Hwang, C.L. and Chandra, S. (1996), *The use of rice husk ash in concrete*, William Andrew Publishing, Westwood, NJ.

Hwang, C.L. and Chen, Y.Y. (1998), "Evaluation of compressive strength of high performance concrete by ultrasonic pulse velocity", *J. Chin Inst. Civil Hydraul Eng*., **10**(3), 591-594.

Hwang, C.L. and Chen, Y.Y. (2002), "The property of self-consolidating concrete designed by desified mixture design algorithm", *Proceeding of First North American Conference on the Design and Use of Consolidating Concrete*.

Hwang, C.L. and Wu, D.S. (1989), "Properties of cement paste containing rice husk ash", *ACI Mater. J.*, **114**, 733-762.

Isaia, G.C., Gastaldini, A.L.G. and Moraes, R. (2003), "Physical and pozzolanic action of mineral additions on the mechanical strength of high-performance concrete", *Cement Concrete Comp*., **25**(1), 69-76.

Kosmatka, S., Panarese, W. and Association, P.C. (1995), *Design and control of concrete mixtures*, Portland Cement Association.

Lee, L.S. and Hwang, C.L. (2002), "A quality assurance system of SCC in Taiwan", *Proceeding of First North American Conference on the Design and Use of Consolidating Concrete*.

Malhotra, V. (2002), "High performance concrete: performance and quality of concrete structures", *Proceedings, Third International Conference*, American Concrete Institute.

Malhotra, V.M. (1976), *Testing hardened concrete: Nondestructure methods*, American Concrete Institute Monograph Series.

Mehta, P.K. (1986), *Concrete-structure, properties and materials*, New York: Prentice-Hall Inc.

Mindess S, Y.J. (1981), *Concrete*, New York: Prentice-Hall Inc.
Mora, C.F., Kwan, A.K.H. and Chan, H.C. (1998), "Particle size distribution analysis of coarse aggregate using digital image processing", *Cement Concrete Res*., **28**(6), 921-932.
Neville, A. (1997), "Water and concrete: A love-hate relationship", *Concrete Int.*, **22**(12), 34-38.
Okamura, H. (1997), "Self Compacting High Performance Concrete", *Concrete Int*., **19**(7), 50-54.
Rodríguez de Sensale, G. (2010), "Effect of rice-husk ash on durability of cementitious materials", *Cement Concrete Comp*., **32**(9), 718-725.
Safiuddin, M., West, J.S. and Soudki, K.A. (2010), "Hardened properties of self-consolidating high performance concrete including rice husk ash", *Cement Concrete Comp*., **32**(9), 708-717.
Salas, A., Delvasto, S., de Gutierrez, R.M. and Lange, D. (2009), "Comparison of two processes for treating rice husk ash for use in high performance concrete", *Cement Concrete Res*., **39**(9), 773-778.
Saraswathy, V. and Song, H.W. (2007), "Corrosion performance of rice husk ash blended concrete", *Constr. Build Mater*., **21**(8), 1779-1784.
Su, N. and Miao, B. (2003), "A new method for the mix design of medium strength flowing concrete with low cement content", *Cement Concrete Comp*., **25**(2), 215-222.
Sumrerng, R. and Prinya, C. (2008), "Mathematical model of strength and porosity of ternary blend Portland rice husk ash and fly ash cement mortar". *Comput. Concrete*, **5**(1), 1-6.
Tsai, C.T., Li, L.S. and Hwang, C.L. (2009), "Durability design and application of steel fiber reinforced concrete in taiwan", *Arab. J. Sci. Eng*., **34**(1B), 57-59.
Zerbino, R., Giaccio, G. and Isaia, G.C. (2011), "Concrete incorporating rice-husk ash without processing", *Constr. Build Mater*., **25**(1), 371-378.
Zhang, M.H., Lastra, R. and Malhotra, V.M. (1996), "Rice-husk ash paste and concrete: Some aspects of hydration and the microstructure of the interfacial zone between the aggregate and paste", *Cement Concrete Res*., **26**(6), 963-977.

*CC*

## Notations

| | |
|---|---|
| $\alpha$ | $\dfrac{w_{fly\ ash}}{w_{cs}+w_{fly\ ash}}$ |
| $\beta$ | $\dfrac{w_{cs}+w_{fly\ ash}}{(w_{cs}+w_{fly\ ash})+w_{ca}}$ |
| $P$ | Theoretical cumulative passing, %. |
| $d$ | Individual sieve size, mm |
| $D$ | Maximum size of the particle, mm. |
| $a_{i,j}$ | (0-1), the retaining portion of $i^{th}$ particle of blended aggregate on the $j^{th}$ sieve. |
| $Pv_i$ | (0-1), the volume percentage of $i^{th}$ particle of blended aggregate, $\%v$ |
| $Pw_i$ | (0-1), the weight percentage of $i^{th}$ particle of blended aggregate ($\%w$) |
| $\gamma_i$ | Bulk specific gravity of the $i^{th}$ particle, kg/m$^3$ |
| $k_j$ | Retaining portion on the $j^{th}$ sieve by theoretical gradation curve |
| $Kss,_j$ | Surface area constant of $j^{th}$ sieve grade, 1/m |
| $Ksst$ | Surface area per kg of blended aggregate, m$^2$/kg |
| $S$ | Total surface area of blended aggregate, m$^2$/m$^3$ |
| $t$ | Coating thickness of lubricating paste on the surface of aggregate, $\mu$m |
| $w_{cs}$ | Weight of fine aggregate per 1 m$^3$ of concrete, kg/m$^3$ |
| $w_{ca}$ | Weight of coarse aggregate per 1 m$^3$ of concrete, kg/m$^3$ |
| $w_c$ | Weight of cement per 1 m$^3$ of concrete, kg/m$^3$ |
| $w_{RHA}$ | Weight of rice husk ash per 1 m$^3$ of concrete, kg/m$^3$ |
| $SP$ | Weight of supperplasticizer 1 m$^3$ of concrete, kg/m$^3$ |
| $w/b$ | Weight ratio of $water/(cement+pozzolans)$ |
| $V_p$ | Total volume of paste, m$^3$ |
| $V_v$ | Total volume of void, m$^3$ |
| $V_a$ | Estimated volume of entrapped air, m$^3$ |
| $U_{\max}$ | The dry loose density under dense state, kg/m$^3$ |